NANOCOMPOSITES OF POLYAMIDE 6, POLYEPICHLOROHYDRIN RUBBER AND ORGANOPHILIC CLAY

C A Pinotti, M I Felisberti*
Chemistry Institute, University of Campinas
PO Box 6154, 13084-971 Campinas, Brazil
*Corresponding author: Tel.: +55 19 3521 3130; Fax: +55 19 3521 3023
Email Address: misabel@iqm.unicamp.br

SUMMARY

Nanocomposites of polyamide 6 toughened with polyepichlorohydrin rubber present improvements in the Young´s modulus and yielding stress, compared with the blend of polyamide 6 and polyepichlorohydrin. The addition of organoclays to the blends can be an important method to control morphology and improve mechanical properties.

Keywords: polyamide 6; nanocomposites; polyepichlorohydrin; blends

1. INTRODUCTION

The discovery of polymeric nanocomposites and supertough blends are clearly the greatest advances in the development of new polymeric materials. Nanocomposites present an increase in stiffness, tensile strength and barrier properties, among others [1,2] while supertough blends combine high impact resistance with ductility [3]. Young's modulus for nanocomposites is significantly higher in comparison to pure polymers. However the temperature of the ductile-brittle transition and the fragility of the material are significantly increased with increases of the clay content. Toughening of nanocomposites with a rubbery disperse phase becomes an interesting alternative to overcome these problems [3]. The toughening of semicrystalline polymers like polyamide 6 (PA6) is well understood and the principal issue for achieving supertough materials is the particle size. Generally, there is an optimum limit for toughening depending on the polyamide and rubber type. It was shown that the dispersed rubber size should be generally controlled between 1 and 0.1 μm to give supertough polyamide materials. But to achieve this appreciable morphology generally are made modifications of either the matrix or the rubber disperse phase. For PA6 toughening the modification of the rubber is more usual and is done by the maleinization process [4]. Polyepichlorohydrin is an elastomeric polymer with a lot of applications, principally in the naval industry. In an earlier work Costa et. al. reported the formation of a graft copolymer in the interface of PA6 and polyepichlorohydrin rubber that can be an important tool for controlling the morphology of blends [5]. Thus, the aim of this work was to prepare and characterize nanocomposites of polyamide 6/organophilic clay toughened with polyepichlorohydrin rubber.

2. Experimental

2.1 Materials

The materials utilized were polyamide 6, PA6 (Invista), polyepichlorohydrin rubber, PEPi (Zeon Chemicals), and two organically modified clays (OMMT): Cloisite 20A (C20A), prepared by an ion exchange reaction between natural sodium montmorillonite (Na-MMT) and dimethyl dihydrogenated tallow, a quaternary ammonium surfactant, and the organoclay Cloisite 30B (C30B), modified with dimethyl dihydrogenated tallow. Both of the OMMT were supplied by Southern Clay Products, Inc. In this study blends of PA6 and PEPi, PA6/PEPi, nanocomposites PA/OMMT and ternary nanocomposites, PA6/PEPi/OMMT were made using the melt blending process.

2.2 Melt Processing

The materials were prepared by melt blending in a corotational and interpenetrating Werner & Pleiderer, Coperion ZSK26, twin-screw extruder (L/D = 48, D = 25 mm) operated at 240 ^{o}C and 300 rpm. The configuration of mixing elements in the extruder is shown in the Figure 1. The 10th zone in Figure 1 represents the vacuum system utilized for the processing of the materials. Firstly, blends with 10 and 20 wt % of polyepichlorohydrin rubber were prepared by adding both materials to the hopper. Nanocomposites with 3 and 5 wt % of C20A and C30B were made by adding PA6 to the hopper and side feeding the organoclays in the 4th zone of the extruder (Figure 1). Adding the organoclay with the side feeder and allowing the polymer to partially melt before the mixing avoids breaking of the clay, which led to shorter particle lengths and a lower matrix reinforcement [6]. For the ternary nanocomposites the blending sequence affects the morphology and consequently the mechanicals properties. For the toughening of the nanocomposites the location of the organoclay in the nanocomposites is a critical question: it is beneficial to have a maximum amount of exfoliated OMMT in the matrix of PA6, and is detrimental having the organoclay located in the rubbery disperse phase because of the reduction of the cavitation ability of the elastomer particles [7]. For the preparation of the ternary nanocomposites three masterbatch were prepared: PA6/PEPi; PA6/C20A and PA6/C30B. After pelletizing the masterbatchs, they were blended together to achieve the desired concentrations in the ternary nanocomposites, that is 5 wt % of the organoclays and 20 wt% of the rubber, both in relation of the mass of PA6. These experimental procedures were for ensuring the preferencial location of the organoclay in the matrix. The nomenclatures used to describe nanocomposites and blends are based on the elastomer and clay contents, respectively. For example, the nanocomposite containing 5 wt% of OMMT C20A is named PA6/5C20A. The blend containing 20 wt% of PEPi is named PA6/20PEPi. The ternary nanocomposite PA6/20PEPi/5C20A contains 20 wt% of PEPi and 5 wt% of OMMT C20A.

All polyamide 6 containing materials were dried in a vacuum oven for 24 h at 90 ^{o}C prior to any melt processing step. The extruded materials were pelletized and then molded into standard tensile (ASTM D638, type I) and flexural (ASTM D790) bars using an Arburg Allrounder 221M 250-55 machine under the following conditions: a barrel temperature of 240 ^{o}C (255 ^{o}C for the nozzle), a mold temperature of 90 ^{o}C, an injection pressure of 800 bars and a holding pressure of 350 bars.

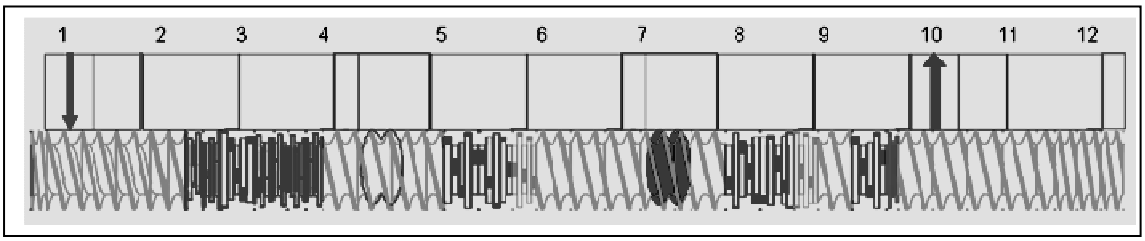

Figure 1: Screw design for the polymer processing.

2.3 Dynamic Mechanical Analysis (DMA)

Dynamic mechanical characteristics of samples in the form of 8 mm x 12.8 mm x 3.2 mm rectangular bars were obtained using a DMTA V Rheometric Scientific equipment operating in the flexural mode at a frequency of 1 Hz, 0.02 % amplitude and a heating rate of 2 ^{o}C/min. The temperature range was between -100 ^{o}C and 220 ^{o}C.

2.4 X-Ray Diffraction (XRD)

The intercalation capability of the polymer into the clay gallery was evaluated by monitoring the interlayer spacing by using an X-ray diffractometer as follows. X-ray diffraction (XRD) analysis of the specimens was carried out using a Shimadzu model XRD 7000 diffractometer (Cu Kα radiation λ = 0.15406 nm) using samples from the tensile bars. Measurements were performed at room temperature in the angular range 2θ = 1^{o}-15^{o}. Interlayer spacings in the nanocomposites were calculated from angular positions of basal reflections *(001)* of the diffratograms using Bragg´s relation: $\lambda = 2d \sin\theta$, where λ corresponds to the wave length of the X-ray radiation used in the diffraction experiment, *d* is the spacing between diffractional lattice planes, and θ is the measured diffraction angle.

2.5 Scanning Electron Microscopy (SEM)

The morphologies of the materials containing polyepichlorohydrin rubber were determined by scanning electron microscopy (SEM) using a JEOL JSM 6360 LV microscope operating with a voltage of 20 kV. The samples were prepared by the cryo fracture of flexural bars in liquid nitrogen and had the rubbery disperse phase extracted with tetrahydrofuran (THF) for 3 hours at room temperature, and then coated with gold for observation. The photomicrographs of SEM were analyzed with an Image ProPlus 4.5 image analyzer to determine the size of the disperse phase. A minimum of 600 dispersed phases were considered to identify the distribution of particle sizes.

2.6 Transmission Electron Microscopy (TEM)

Ultra thin sections for TEM analysis, approximately 45 nm thickness, were cut from flexural bars, in the section perpendicular to the flow direction, with a diamond knife at a temperature of -100 ^{o}C using a Leica UC6 ultracut microtome. Some samples were

examined by TEM using a Carl Zeiss CEM 902 microscope with a field emission gun at an accelerating voltage of 80 kV.

2.7 Mechanical Testing

Tensile tests were conducted at room temperature according to ASTM D638 using an EMIC DL 2000 machine. Yield strength and elongation at break were measured at the crosshead speed of 50 mm/min while the Young´s modulus was measured using an extensometer and a crosshead speed of 5 mm/min. Three point flexural tests were conducted according ASTM D790 with a crosshead speed of 5.3 mm/min. The tensile, flexural and impact property values reported here represent the average from a minimum of 8 samples. Standard notched Izod impact tests were performed on the 3.2 mm thick Izod bars using a Tinius Olsen 899 machine according to ASTM D256 at the temperature of 23 ± 2 ^{o}C. Before the mechanical tests the samples were kept in desiccators for a minimum of 48 hours.

3. Results and Discussion

Figure 2 shows the storage modulus (E´) and loss modulus (E´´) obtained from DMA for the materials. The glass transition temperature, T_g, was taken as the maximum of E´´ *versus* T curves.

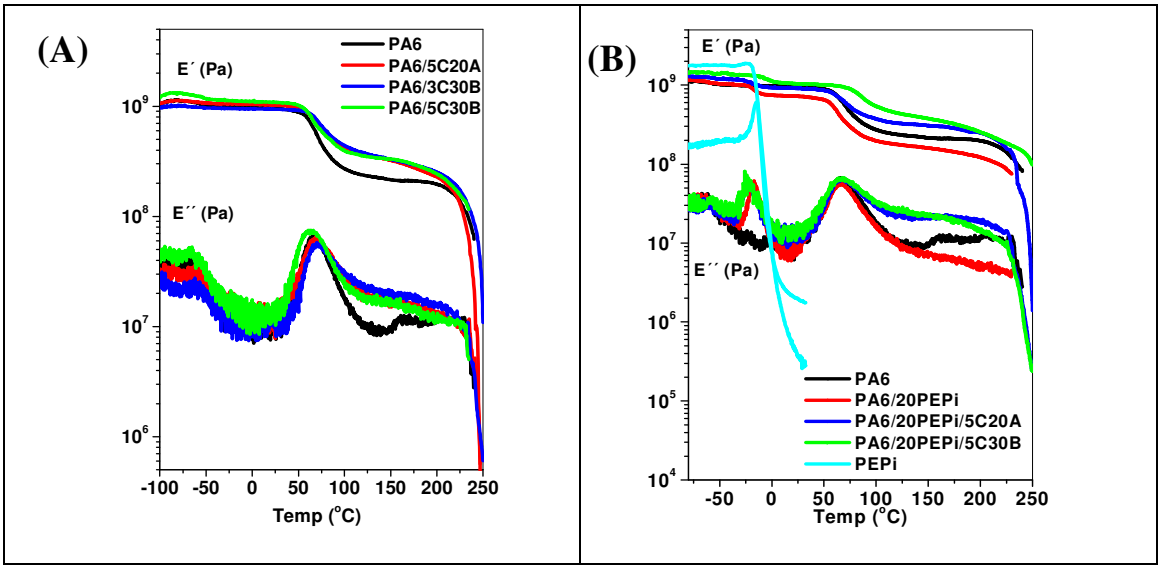

Figure 2: Storage modulus E´ (MPa) and loss modulus E´´ versus temperature for: (A) Nanocomposites and (B) Blends and ternary nanocomposites.

The E´´xT curves for PA6 present two maximum: one at approximately -65 ^{o}C related to the β relaxation of the hydrogen bonded amide group and another at 65 ^{o}C, corresponding to the T_g of the polyamide [8]. PEPi rubber presents a maximum in the E´´xT at -17 ^{o}C, and for the blends and ternary nanocomposites a maximum at -23 ^{o}C, related to the T_g of the elastomeric phase. The curves of the storage modulus, E´ *versus*

temperature, of the blends and the ternary nanocomposites demonstrate the immiscibility between PA6 and the rubber and the morphology of a disperse phase of PEPi in the PA6 matrix. For the nanocomposites the storage moduli is always higher than the neat PA6 above 65 ^{o}C, the T_g of the matrix.

The X-ray diffratograms of the materials are presented in the Figure 3. The OMMT pattern shows intense peaks at around $2\theta = 3.6^{o}$, corresponding to a basal spacing (d_{001}) of 2.4 nm for the organoclay C20A (Figure 3A) and a $2\theta = 4.9^{o}$ for C30B corresponding to a d_{001} of 1.8 nm (Figure 3B). For the nanocomposites with 3 and 5 wt % of C20A, PA6/3C20A and PA6/5C20A, respectively, the patterns presented a shift of the basal spacing to 3.5 and 3.6 nm, demonstrating a typical morphology of intercaled nanostructures. These shifts are also observed for the nanocomposites with the organoclay Cloisite 30B, PA6/3C30B and PA6/5C30B (Figure 3B).

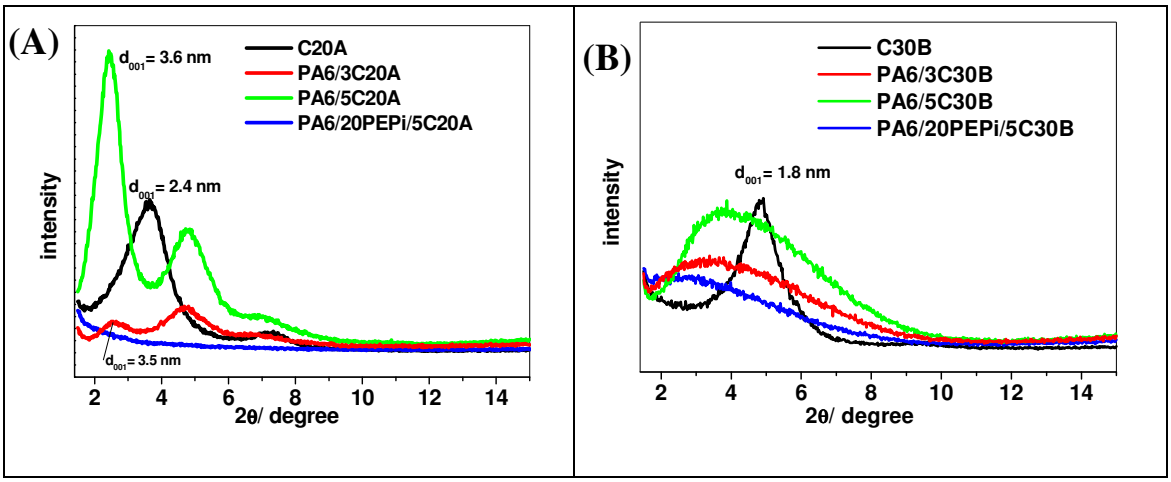

Figure 3: X-ray diffraction patterns for the organoclays, nanocomposites and ternary nanocomposites.

For the ternary nanocomposite PA6/20PEPi/5C20A the diffraction pattern is typical of a well-exfoliated nanocomposite, which is desired from the point of view of mechanical and barrier properties. For PA6/20PEPi/5C30B the diffraction pattern is typical of exfoliated with a presence of some clay tactoids in the nanocomposite, which presents a large reduction in intensity and a shift of the diffraction peak.

The morphology of the materials containing polyepichlorohydrin rubber were analysed by SEM. Figure 4 shows micrographs of the blends with 10 and 20 wt% of rubber that represent the morphology of a rubber phase dispersed by the PA6 matrix. The voids in the micrographs correspond to the elastomer phase, which was extracted with tetrahydrofuran. The distribution of the particle sizes is also demonstrated in the Figure 4. The averages of the particles sizes were 0.4 and 0.5 μm for the blends PA6/10PEPi and PA6/20PEPi, respectively.

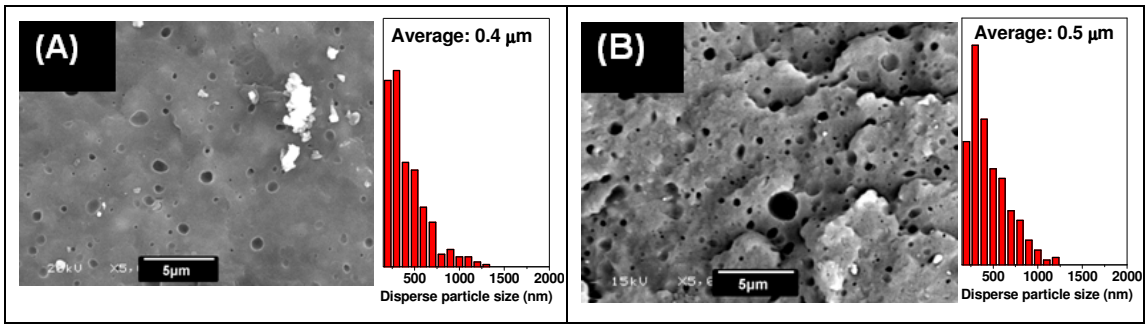

Figure 4: SEM micrographs of the cryo fracture of the samples after extraction of the elastomer phase of (A) PA6/10PEPi and (B) PA6/20PEPi, and distributions of the disperse phase size.

The SEM micrographs and distributions of the elastomer particle sizes of the ternary nanocomposites is shown in Figure 5. It can be noted that the incorporation of the organoclays influenced the morphology of the elastomer disperse phase, causing a reduction in the particles sizes and improving uniformity of the distribution of the particles in the matrix. The average particle sizes for PA6/20PEPi/5C20A and PA6/20PEPi/5C30B were 0.3 µm.

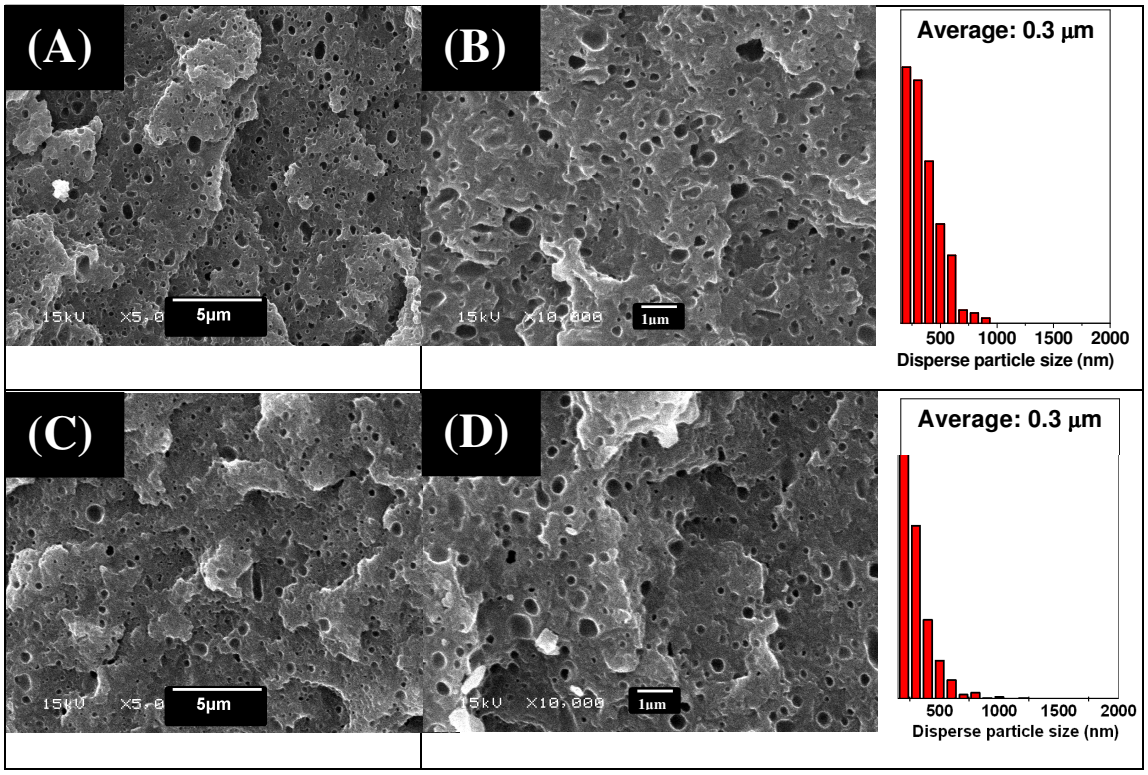

Figure 5: SEM micrographs of the cryo fracture of the samples after extraction of the elastomer phase of (A) and (B) PA6/20PEPi/5C20A and (C) and (D) PA6/20PEPi/5C30B, and distributions of the disperse phase sizes.

The presence of organoclay and an increase in clay content causes a decrease in the rubber particle size. The presence of platelets of the OMMT may act like a physical barrier to prevent coalescence of the rubber domains and thus decrease the rubber

particle size, which is desirable for toughening of the matrix, since there will be a larger number of disperse phases and the inter particle distance will be lower [9].

In order to study the morphology and to evaluate the degree of exfoliation of the organoclay in the nanocomposites transmission electron microscopy (TEM) was used. A TEM micrograph for the ternary nanocomposite PA6/20PEPi/5C30B is shown in Figure 6.

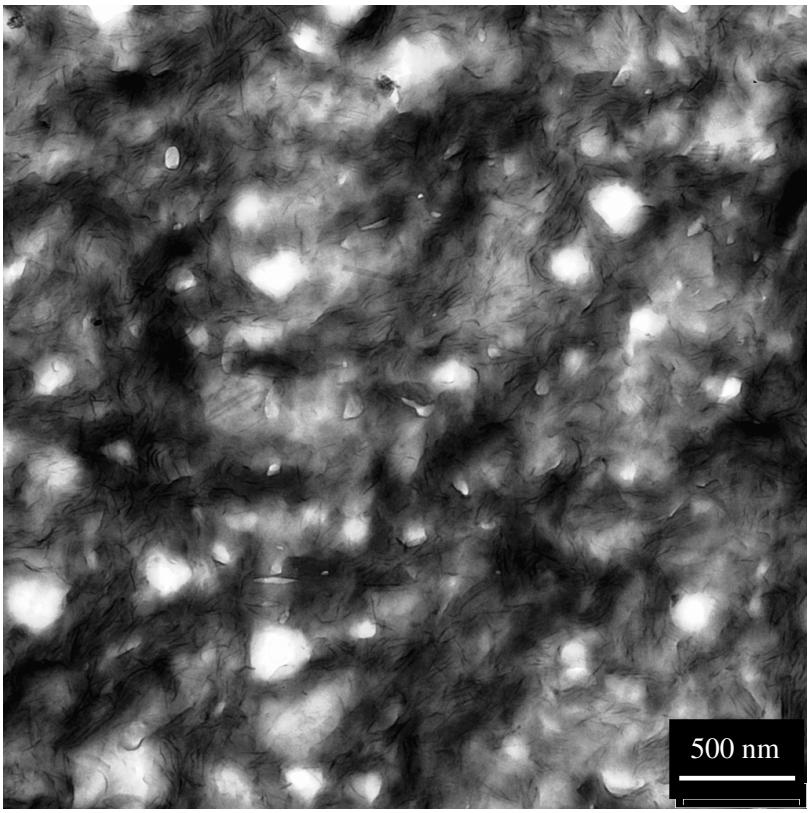

Figure 6: TEM microphaphs of the ternary nanocomposite PA6/20PEPi/5C30B.

The micrograph confirms the morphology of dispersed phase elastomer in the PA6 matrix, where the white phase is the rubbery phase. Moreover a high degree of exfoliation with the presence of some organoclay tactoids can be observed (dark phases), in agreement with the XRD analysis. The location of the clay platelets is preferably on the PA6 matrix, which is desirable for the toughening of the nanocomposites.

Tables 1 and 2 present the mechanical properties for neat PA6, the blends with PEPi, and the ternary nanocomposites.

Table 1: Tensile properties for the materials and the relation of gain (+) or loss (-) in properties in percent (%) in relation to neat PA6.

Material	Yielding stress (MPa)	Young´s modulus (GPa)	Elongation at break (%)
PA6	73 ± 1	2,63 ± 0,06	27 ± 9
PA6/20PEPi	51 ± 1 (-30%)	1,88 ± 0,05 (-29%)	65 ± 13 (+141%)
PA6/20PEPi/5C20A	71 ± 1 (-3%)	2,88 ± 0,06 (+10%)	11,4 ± 0,7 (-58%)
PA6/20PEPi/5C30B	77 ± 2 (+5%)	3,14 ± 0,06 (+19%)	6,7 ± 0,8 (-75%)
PA6/3C20A	80,1 ± 0,7 (+10%)	3,1 ± 0,2 (+18%)	-
PA6/5C20A	82,7 ± 0,3 (+13%)	3,24 ± 0,05 (+23%)	6,3 ± 0,4 (-77%)
PA6/3C30B	103 ± 1 (+41%)	3,75 ± 0,06 (+43%)	-
PA6/5C30B	110 ± 2 (+51%)	4,22 ± 0,07 (+60%)	5,5 ± 0,4 (-80%)

Table 2: Flexural and impact properties for the materials and the relation of gain (+) or loss (-) in properties in percent (%) in relation to neat PA6.

Material	Flexural modulus (MPa)	Yielding flexural stress (MPa)	Notched Izod Impact (J/m)
PA6	2,63 ± 0,06	73 ± 1	52 ± 4
PA6/20PEPi	1,88 ± 0,05 (-29%)	51 ± 1 (-30%)	712 ± 45 (+1269%)
PA6/20PEPi/5C20A	2,88 ± 0,06 (+10%)	71 ± 1 (-3%)	73 ± 8 (+40%)
PA6/20PEPi/5C30B	3,14 ± 0,06 (+19%)	77 ± 2 (+5%)	73 ± 5 (+40%)
PA6/3C20A	3,15 ± 0,04 (+20%)	80 ± 1 (+10%)	40 ± 3 (-23%)
PA6/5C20A	3,24 ± 0,05 (+23%)	82,7 ± 0,3 (+13%)	37 ± 4 (-29%)
PA6/3C30B	3,75 ± 0,06 (+43%)	103 ± 1 (+41%)	38 ± 5 (-27%)
PA6/5C30B	4,22 ± 0,07 (+60%)	110 ± 2 (+51%)	37 ± 2 (-29%)

The addition of the rubbery phase to the PA6 matrix leads to a significant improvement of the impact resistance of the material (712 ± 45 J/m), leading to a super tough material. In contrast the yield stress and Young´s modulus is reduced about 30% in relation to neat PA6.

The incorporation of organoclay in PA6 results in a significant improvement in the yielding stress and flexural modulus, however it results in a decrease in the impact resistance, which can be resolved by introducing a rubbery disperse phase. The ternary nanocomposites presented intermediate properties between the nanocomposites and the blend with PEPi, presenting a synergetic effect in relation to the neat PA6, increasing both modulus and impact resistance. The incorporation of the organoclay caused a large reduction in the impact strength, when comparing the blend and the ternary nanocomposite, which can be caused by a blocking effect on overlap of the stress volume of the disperse rubbery phase [10].

4. Conclusion

In this study, blends, nanocomposites and a ternary nanocomposite of PA6, montmorillonite organoclays and polyepichlorohydrin rubber were prepared. The XRD provided evidence of the exfoliation of the clay in the ternary nanocomposites and the TEM micrographs showed the preferable location of the platelets in the matrix of PA6, which is so desirable from the mechanical point of view. The blend with 20 wt % of

PEPi is a super tough material, however its impact strength decreases with the addition of the organoclay in the ternary nanocomposites. The SEM analysis demonstrated the influence of the incorporation of the clay in the ternary nanocomposites on the morphology of the rubbery disperse phase. The presence of the clay platelets promoted a reduction in the average sizes and a better uniformity in the distribution of dispersed particle sizes, indicating that the formation of lamellar nanocomposites can be a good alternative to control morphology of immiscible systems.

ACKNOWLEDGEMENTS

The authors are grateful to Dr. C. H. Collins for manuscript revision and to CNPq and FAPESP for the financial support.

5. Reference

1. W. S. Chow, A. A. Bakar, Z.A.M. Ishak, J. Karger-Kocsis, and U.S. Ishiaku, European Polymer Journal, **41**, 687, (2005).
2. P. C. LeBaron, Z. Wang, and J. Pinnavaia, Applied Clay Science, **15**, 11 (1999).
3. Y.-C. Ahn, and D.R. Paul, Polymer, **47**, 2830, (2006).
4. A. J. Oshinski, H. Keskkula, and D. R. Paul, Polymer, **33,** 268, 1992.
5. S. C. Goos, M. C. Gonçalves, and M. I. Felisberti, Journal of Applied Polymer Science, **72**, 1827, (1999).
6. F. Chavarria, R. K. Shah, D. L. Hunter, and D. R. Paul, Journal of Polymer Engineering and Science, **47**, 1847, (2007).
7. A. Dasari, Z. Z. Yu, and Y. W. Mai, Polymer, **46**, 5986, (2005).
8. S. C. Goos, and M. I. Felisberti, Journal of Applied Polymer Science, **72**, 1835, (1999).
9. I. Gonzalez, J. I. Eguiazabal, and J. Nazabal, Composites Science and Technology, **66**, 1833, (2006).
10. K. Wang, C. Wang, J. Li, J. Su, Q. Zhang, R. Du, and Q. Fu, Polymer, **48**, 2144, (2007).

Previous Paper *Back to Programme* *Back to Topic*